

# Molecular association of normal alkanolic acids with their thallium(I) salts: a new homologous series of fatty acid metal soaps

M. Fernández-García,<sup>1,\*</sup> M. V. García,\* M. I. Redondo,\* J. A. R. Cheda,\* M. Fernández-García,<sup>2,\*</sup> E. F. Westrum, Jr.,<sup>†</sup> and F. Fernández-Martín<sup>3,§</sup>

Departamento de Química Física I,\* Universidad Complutense, Madrid, Spain; Department of Chemistry,<sup>†</sup> University of Michigan, Ann Arbor, MI 48109; and Instituto del Frio (CSIC),<sup>§</sup> Ciudad Universitaria, 28040 Madrid, Spain

**Abstract** A new homologous series of thallium(I) hydrogen dialkanoates, fatty acid thallium soaps, from the dipropane up to the ditetradecane is reported for the first time. This association with 1:1 stoichiometry is the only one exhibited by the thallium derivatives. They have been prepared by solidification of molten mixtures with equimolar proportions of acid and corresponding neutral salt, although crystallization from an anhydrous ethanolic solution of the mixture has also been successful in getting pure compounds with largest chain lengths. Vibrational spectroscopies clearly characterize these crystalline compounds as very strong hydrogen bonding systems. Assignations of active modes in proton and carbon nuclear magnetic resonance spectrometry (NMR) (in ethanol) and infrared (IR) and Raman spectra (in solid state) are reported. According to X-ray diffraction (XRD) they have monomolecular lamellar structures with the acyl chains arranged up and down to the cation/H-bond network in a methyl-to-methyl fashion, and vertically oriented to the basal plane. The acyl chains present all-*trans* conformation and alternating configuration (perpendicular orthorhombic subcell), like the  $\beta'$ -phases of other kinds of lipids. Lamellar thickness is reported for the six room-temperature crystalline members. The molecular compounds present polymorphism, one crystal/crystal transition at temperatures close to the peritectical melting. Phase transition thermodynamics are also given and discussed with respect to their acid and salt parents. Their incongruent melting involves nearly 90% of the total enthalpic increments of both constituents' melting processes, making these compounds potential thermal energy storage materials.—Fernández-García, M., M. V. García, M. I. Redondo, J. A. R. Cheda, M. Fernández-García, E. F. Westrum, Jr., and F. Fernández-Martín. Molecular association of normal alkanolic acids with their thallium(I) salts: a new homologous series of fatty acid metal soaps. *J. Lipid Res.* 1997. **38**: 361–372.

**Supplementary key words** thallium(I) • hydrogen dialkanoates • thermodynamics of phase transitions • CH<sub>2</sub> conformation-configuration-packing • lamellar structures • energy storage materials • differential scanning calorimetry • fourier transform infrared spectroscopy • nuclear magnetic resonance spectrometry • Raman • X-ray diffraction

Fatty acids and neutral alkali soaps are known to bond by fairly strong hydrogen bonds, yielding crystalline molecular associations (metal hydrogen dialkanoates, colloquially, but incorrectly, termed metal acid alkanates or, in general, fatty acid soaps) in the anhydrous state either by cooling the melt of stoichiometric amounts of the components (1) or by crystallizing from a proper solution of the mixed components (2), but also in the presence of moderate amounts of water in corresponding aqueous ternary system (3). Although hydrated forms have also been reported (4), three-compound aggregates are to be considered rather than true hydrated acid soaps (5). Recent updated revisions on anhydrous sodium and potassium acid soaps and acid soaps–water systems have been published by Stenius and Ekwall (6), Small (7), and Mantsch et al. (8).

Normal chain sodium alkanates, for instance, often show the formation of different molecular compounds of several stoichiometries (acid:soap molar ratios of 3:2, 1:1, 2:3, 2:5, 1:5) and, as a general rule, the acid-rich compounds exhibit polymorphism (two crystal/crystal transitions at most) and melt incongruently yielding the next more soap-rich compound, while the salt-rich ones melt congruently and reveal lyotropic behavior by passing through several mesomorphic phases before clearing into the isotropic liquid (9–14). On the other hand,

Abbreviations: TMS, tetramethyl silane; DSC, differential scanning calorimetry; FTIR, fourier transform infrared spectroscopy; GLC, gas–liquid chromatography; MC, molecular compound; NMR, nuclear magnetic resonance spectrometry; XRD, X-ray diffraction.

<sup>1</sup>Present address: Marcos F-G; Instituto de Catálisis y Petroleoquímica (CSIC), Campus Cantoblanco, 28049 Madrid, Spain.

<sup>2</sup>Present address: Marta F-G; Instituto de Ciencia y Tecnología de Polímeros (CSIC), 28006 Madrid, Spain.

<sup>3</sup>To whom correspondence should be addressed.

only equimolecular complexes have been reported for the fatty acid potassium soaps (1, 15–17). Other fatty acid alkali soaps have received much less or no attention presumably in correspondence with that devoted to the study of the respective homologous series of the neutral alkali (Li, Rb, Cs) salts (18).

Acid thallium(I) alkanates have remained unknown until the report of the existence of an equimolecular compound in the heptanoic + heptanoate system (19) and the subsequent finding that this is a common phenomenon for shorter and longer, odd and even normal members of the acid and soap homologous series from 3 to 14 carbon atoms in both acyl chains (20).

This paper presents for the first time a general description of the new homologous series of normal thallium(I) hydrogen dialkanates, fatty acid thallium soaps, concerning their structural and thermodynamic characterization. The structural description includes their spectroscopic behavior, by reporting nuclear magnetic resonance spectrometry (NMR), fourier transform infrared spectroscopy (FTIR), and Raman data, as well as powder X-ray diffraction. The different information obtained is combined and discussed to reveal the nature of the chemical association and the type of structure originated, as well as the kind of internal order that the alkyl chains and the “head groups” present in it. Their thermal behavior studied by differential scanning calorimetry (DSC) constitutes the thermodynamic characterization of phase transitions. Comparisons are made to other homologous series of lipids, particularly the fatty acids and the thallium(I) salts involved.

## MATERIALS AND METHODS

### Sample provenance

Anhydrous thallium(I) acid soaps from the propanoic-propanoate (MC3) to the tetradecanoic-tetradecanoate (MC14) members were prepared by mixing equimolar amounts of the corresponding constituents, melting the mixture, and grinding it to a fine powder that, after careful mixing, was melted and reground to attain homogeneity. Liquid fatty acids were used as received (Fluka puriss grade,  $\geq 99.5\%$ ) and after recrystallization from anhydrous ethanolic solution and vacuum-drying in the case of crystalline products; GLC analysis of the methyl esters resulted in around 99.8% wt as typical purity (19). Thallium(I) alkanates were prepared by heterogeneous reaction between the corresponding acid in anhydrous methanol (Fluka purum grade) and thallium(I) carbonate (Fluka puriss grade,  $\geq 99\%$ ), according to the method described elsewhere

(21). After double recrystallization in anhydrous ethanol (purum) and room temperature vacuum-drying, the salts showed over 99.7 molar percent purity as evaluated by convectional DSC fractional fusion techniques.

Anhydrous molecular compounds (MC) were also obtained by crystallization from an anhydrous ethanolic solution of the corresponding constituents in equimolar proportions. However, in spite of trying other stoichiometries and checking several temperatures, the yield always contained small amounts of free salt; only the MC12 and, particularly, MC14 members of the series were obtained nearly free of this contamination. The co-crystallized salt retains its identity as long as the MC melting does not occur, so its presence can be detected and quantitatively estimated from the corresponding crystal/crystal transition in the DSC heating trace. On cooling the melted system, the MC crystal, depending on the chain lengths involved, may incorporate the salt excess by forming solid solutions, hence subsequent DSC heating traces are not useful for purity determination.

Caution must be taken in handling the lowest MC members due to the high hygroscopicity observed by the corresponding solid salts and, particularly, liquid acids.

### Nuclear magnetic resonance (NMR)

$^1\text{H}$  and  $^{13}\text{C}$  NMR spectra of the solutions in deuterated chloroform ( $\sim 0.3\text{ M}$ ) were recorded on a Varian Gemini 200 NMR Spectrometer (Varian Associates Inc., Palo Alto, CA), operating at 200 MHz under the following conditions: pulse repetition time, 1 s; probe temperature, 25°C; reference, central peak of  $\text{CDCl}_3$  assigned as 7.24 ppm and 77.0 ppm, respectively, with reference to TMS.

### Vibrational spectroscopies (FTIR and Raman)

FTIR spectra were recorded on a Nicolet 60SX system (Nicolet Instrument Corporation, Madison, WI) at a nominal resolution of  $2\text{ cm}^{-1}$ , and 50 scans averaging for good signal/noise ratio. Temperature dependence was studied by using a Specac VTL-2 variable temperature cell (Graseby-Specac Ltd., Kent, U.K.) on powder samples sandwiched between TlBr pellets, as metathesis ( $\text{K}^+$  and  $\text{Tl}^+$  ion interchange) was detected when KBr pellets were used in the traditional method. The 514.5 nm  $\text{Ar}^+$  and 647.1 nm  $\text{Kr}^+$  lines from two Innova 70 lasers (Coherent Laser Product Division, Palo Alto, CA) were used to produce the Raman effect and the spectra were recorded with a Dilor XY instrument (Dilor S.A., Lille, France). Spectral slit width was  $5\text{--}3\text{ cm}^{-1}$  and integration time varied 4–20 sec, depending on the Raman signal intensities.

## X-ray diffraction (XRD)

Powder XRD at  $0.5^\circ \leq 2\theta \leq 50^\circ$ ,  $\Delta(2\theta) = 0.05^\circ$ , counting time = 2.0 s, was carried out at room temperature on solid MC samples by means of a computerized Siemens Kristalloflex X-ray generator and D5000 diffractometer (Siemens AG, Karlsruhe, Germany), using Ni-filtered  $\text{CuK}\alpha$  radiation ( $\lambda = 1.5418 \text{ \AA}$ ).

## Differential scanning calorimetry (DSC)

DSC measurements were carried out with a Perkin-Elmer DSC2C equipped with cooling unit Intracooler II and TADS3700 Data Station (Perkin-Elmer, Norwalk, CT). Temperature response was calibrated along the entire temperature range of interest through the melting points of high purity chemicals (undecane, tridecane, pentadecane, gallium, lauric and stearic acids, and indium). Energetic response was calibrated by the enthalpy of melting of 99.999% pure indium. Each compound, in amounts of 10–15 ( $\pm 0.002$ ) mg by a Perkin-Elmer Autobalance AD4, was sampled 6 times. Data were obtained from heating runs usually scanned at 1 K/min heating rate. Temperatures and enthalpy values are considered to be reliable within standard deviations better than  $\pm 0.5 \text{ K}$  and  $\pm 3\%$ , respectively.

## RESULTS

### NMR spectra

Typical spectra in solution of (dodecanoic) lauric acid, thallium(I) laurate, their equimolar physical mixture, and the corresponding molecular association MC12 are shown in Fig. 1, the groupings and positions in all the samples presenting the typical pattern of straight chain lipids (22, 23). The spectrum essentially records four groupings in all the cases that, as signal positions shift downfield, can be identified as pertaining to the terminal methyl group (triplet), the ordinary methylene groups of the normal chain (C(4)–C(11), complex and largest peak), the methylene corresponding to the third carbon atom ( $\beta\text{-CH}_2$ , quintet), and the methylene adjacent to the carboxyl group ( $\alpha\text{-CH}_2$ , triplet), respectively. The broad signal of the carboxylic hydrogen in the fatty acid appeared around 11.08 ppm (strongly affected by the concentration, it does not give the specific position of the peak; not shown in Fig. 1). Signals belonging to the first two groupings, protons in chain carbons C(4)–C(12), remained practically unaltered when passing to the other three samples; the major variations recorded affect both C(2) and C(3) methylene groups, whose signals were shifted upfield in the soap because of the introduction

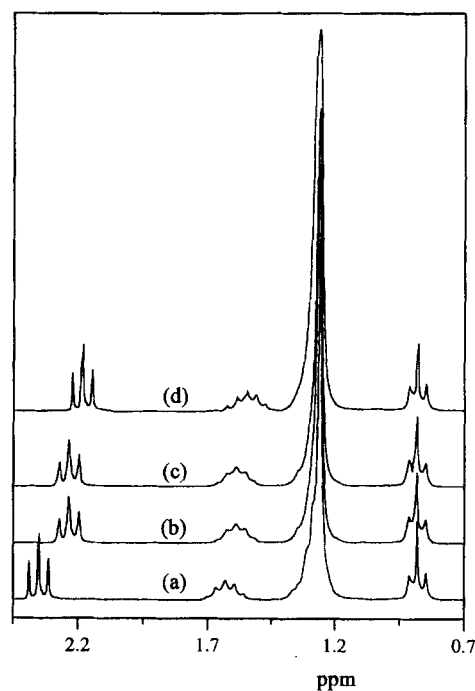


**Fig. 1.** Proton resonance spectra of the lauric series in solution: (a) dodecanoic acid; (b) acid + salt mixture; (c) thallium(I) hydrogen didodecanoate (MC12); (d) thallium(I) dodecanoate.

of the thallium(I) cation which is more electropositive than the acidic proton. Physical mixtures and acid soaps came out amidst the corresponding acid and salt signals, indicating an electronegative character intermediate between those of the carboxylic and carboxylate groups for the chemical environment. On the other hand, the carboxylic proton signal was sharpened and shifted downfield to around 11.40 ppm in the mixture and in the molecular association compared to that of the acid, indicating a stronger interaction than in the dimeric acid. Additionally, the signal consisted of a single signal with smooth downfield skewness indicating a chemical environment rather comparable for the carboxylic and carboxylate moieties. In agreement with the signal of the proton, the two  $\alpha$  methylene groups (acid and salt alkyl chains) yielded a single signal in the mixture and molecular compound. A single signal was also produced by the two  $\beta$  methylenes. This behavior is substantially similar to the case of liquid samples of sodium caprylate in caprylic acid (4). The corresponding signals can be approximately centered at the positions given in Table 1.

Similar behavior was detected in the case of the carbon resonance spectra, as can be seen in Fig. 2 that also displays the lauric series as a typical example of all the systems studied. Signal positions corresponding to C(1), C(2), C(10), C(3), C(11), and C(12) appear

TABLE 1. NMR chemical shift data from proton resonance spectra on the lauric series

Acid	$\delta$ (ppm)			Assignment
	Mixture	Mol. Assoc.	Salt	$^1\text{H}$
0.88	0.88	0.88	0.88	$-\text{CH}_3$
1.2-1.4	1.2-1.4	1.2-1.4	1.2-1.4	$-\text{CH}_2^a$
1.63	1.60	1.60	1.55	$\beta\text{-CH}_2-$
2.35	2.22	2.22	2.17	$\alpha\text{-CH}_2-$
11.08 <sup>b</sup>	11.40 <sup>b</sup>	11.40 <sup>b</sup>	—	$-\text{COOH}$

<sup>a</sup>Methylene groups from C(4) to C(11).

<sup>b</sup>Concentration dependent, not in specific position.

clearly separated and shifted highfield. Those belonging to C(5), C(6), and C(7), and to C(4), C(8), and C(9) appear closely grouped around 29.6 ppm, sided highfield and downfield respectively, as **Table 2** shows. Consistent with previous data on proton resonance, the signals corresponding to carbon atoms C(4) to C(12) remained practically unaltered while those from C(1), C(2), and C(3) appeared between the respective acid and salt positions. In addition, a single signal was recorded for the two carbonyl groups at about 180.85 ppm indicating the chemical equivalence between them (symmetric H-bond for the molecular compound in solution), as well as its proximity to that of acid dimers in solution. Single signals were recorded for the carbon atoms of each couple of  $\alpha$  and  $\beta$  methylene

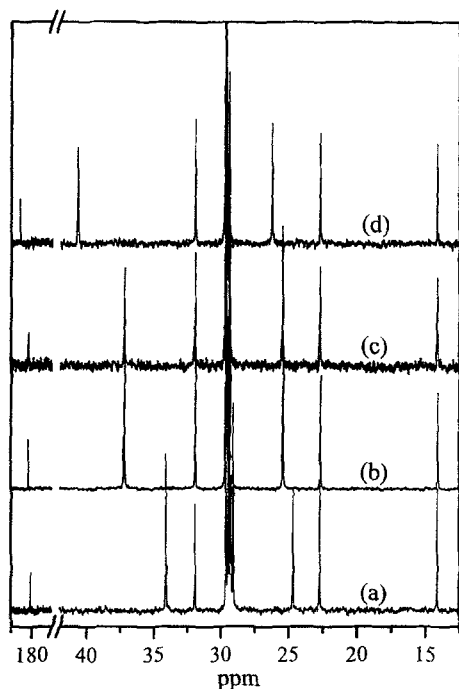


Fig. 2. Carbon resonance spectra of the lauric series in solution: (a) dodecanoic acid; (b) thallium(I) hydrogen didodecanoate (MC12); (c) acid + salt mixture; (d) thallium(I) dodecanoate.

TABLE 2. NMR chemical shift data from carbon resonance spectra on the lauric series

Acid	$\delta$ (ppm)			Assignment
	Mixture	Mol. Assoc.	Salt	$^{13}\text{C}$
14.12	14.13	14.14	14.15	C(12)
22.65	22.71	22.71	22.70	C(11)
31.91	31.94	31.99	31.93	C(10)
29.24	29.44	29.42	29.59	C(9)
29.43	29.58	29.56	29.66	C(8)
29.59	29.67	29.67	29.70	C(7)
29.59	29.67	29.67	29.70	C(6)
29.33	29.44	29.42	29.66	C(5)
29.06	29.38	29.38	29.42	C(4)
24.67	25.47	25.47	26.24	C(3)
34.08	37.25	37.43	40.68	C(2)
180.28	180.83	180.86	182.93	$\text{C}=\text{O}$

groups indicating the equivalence among alkyl, acid, and salt chains in the molecular compound. Identical spectra for the equimolar physical mixture and the molecular association in solution were also observed here.

### IR spectra

Infrared spectra of crystalline compounds presented the characteristic pattern of an alkyl chain in addition to bands due to the carboxyl moieties, as shown in **Fig. 3**, where the IR spectrum of the lauric-laurate association MC12 is presented between 500 and 2000  $\text{cm}^{-1}$  together with the very different composite spectrum computed from the individual spectra of lauric acid and thallium(I) laurate in equimolar proportions. The lack of  $\nu(\text{OH})$  stretching bands in the 2500-3500  $\text{cm}^{-1}$  region of the crystalline molecular compounds spectrum

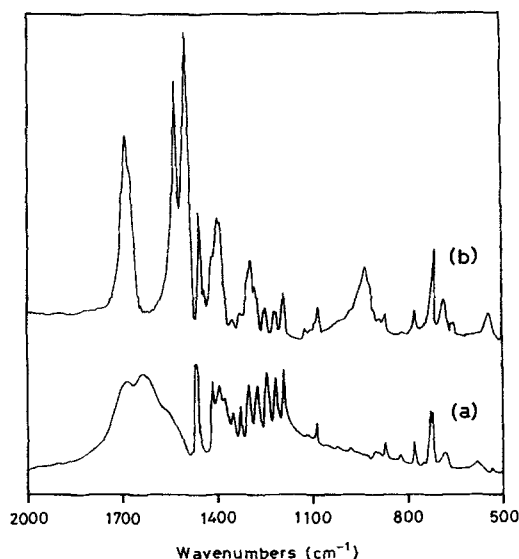
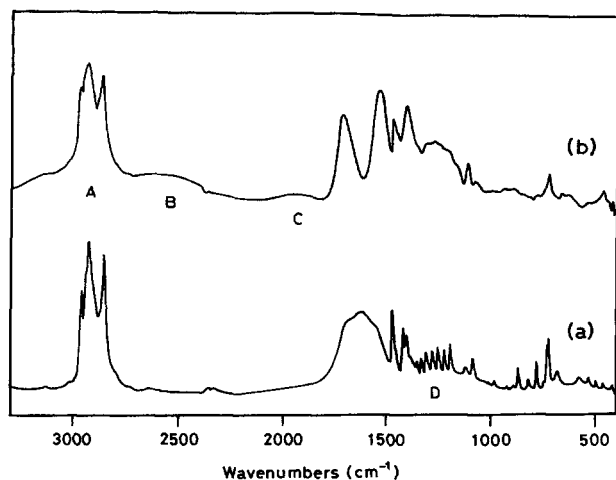


Fig. 3. Infrared spectrum of the thallium(I) hydrogen didodecanoate (lauric-laurate association MC12): (a) experimental; (b) calculated for the physical acid + salt mixture.



**Fig. 4.** Effect of temperature on the IR spectra of thallium(I) hydrogen didodecanoate (lauric-laurate association MC12), showing the A, B, and C bands onset, and disappearance of the D band: (a) crystalline sample at 30°C; (b) molten sample at 65°C.

was replaced by an absorption continuum shifted to the 1100–1400  $\text{cm}^{-1}$  region on which the progression bands appeared.

The temperature dependence of the spectral evolution over the frequency range 400–3500  $\text{cm}^{-1}$  is shown in **Fig. 4** to illustrate the melting process of the MC12 complex. Of particular interest are the changes observed in the 1600  $\text{cm}^{-1}$  vibration zone, associated with the antisymmetric stretching modes of the carboxylate moiety, as well as the disappearance of the fine structure at the melting temperatures.

### Raman spectra

A typical Raman spectrum of the crystalline compounds is shown in **Fig. 5**, where that of the myristic-myristate association MC14 is compared with the direct sum of the myristic acid and thallium(I) myristate spectra in equimolar ratio. Some differences between acid and salt constituents and equimolecular compound were observed in the Raman bands around 1450  $\text{cm}^{-1}$ , particularly in the intensity ratio between bands at 1460 and 1440  $\text{cm}^{-1}$ , related to the crystalline chains packing symmetry; other subtle but distinctive facts will be discussed later. Absorption bands are assigned to the respective IR and Raman active modes in **Table 3**. No significant position differences were found between samples crystallized from ethanol or solidified from the melt.

### XRD

Powder XR diffractograms of crystalline molecular associations at about 15°C presented a series of more than 20 orders of reflections, very sharp in the low angle region, with gradual decay in intensity (no transforma-

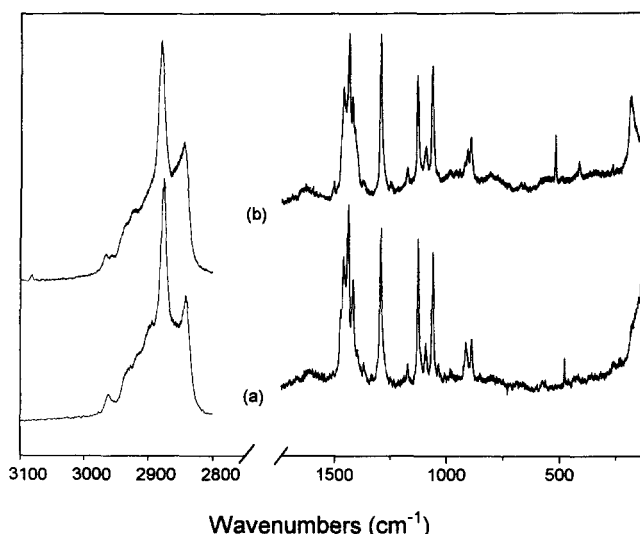


**Fig. 5.** Raman spectrum of the thallium(I) hydrogen ditetradecanoate (myristic-myristate association MC14): (a) experimental; (b) calculated for the physical acid + salt mixture.

tions were detected in the experiment, however). Moreover, a slight weakening of the even order reflections (Shearer effect) was found similar to that observed in alkyl iodides (24), which disappeared at a certain order (13th for MC9, 18th for MC14), and which displayed

**TABLE 3.** Vibration modes assignment to IR and Raman absorption bands in thallium(I) hydrogen dialkanoates

Bands ( $\text{cm}^{-1}$ )		
IR <sup>c</sup>	Raman <sup>c</sup>	Mode <sup>a,b</sup>
2955	2960	$\nu_s(\text{CH}_3)$
2910	2878	$\nu_s(\text{CH}_2)$
2865	—	$\nu_s(\text{CH}_3)$
2848	2844	$\nu_s(\text{CH}_2)$
1686	1615	$\nu_s(\text{COO})$
1625		
1548		
1470, 1465		
—	1457, 1441	$\delta(\text{CH}_2)$
—	1419	
—	1403	$\nu_s(\text{COO})$
1378	—	$\delta(\text{CH}_3)$
—	1294	t( $\text{CH}_2$ )
—	1174	r( $\text{CH}_2$ )
—	1125	$\nu_s(\text{CC})$
1330–1100	—	w( $\text{CH}_2$ )
—	1060	$\nu_s(\text{CC})$
728, 720	—	r( $\text{CH}_2$ ) all in phase
—	914	r( $\text{CH}_3$ ) and
—	890	terminal $\nu_s(\text{CC})$
700–100	—	r( $\text{CH}_2$ )
679	—	$\delta(\text{COO})$
578	—	w( $\text{COO})$

<sup>a</sup>w, wagging; t, twisting; r, rocking;  $\nu_s$ , symmetric stretching;  $\nu_a$ , antisymmetric stretching;  $\delta$ , scissoring;  $\gamma$ , out of plane deformation.

<sup>b</sup>No IR bands assigned to  $\nu(\text{OH})$  mode are observed but continuous absorption along the 1100–1400  $\text{cm}^{-1}$  range.

<sup>c</sup>Band couples denote group splitting due to intermolecular interactions in the O $\perp$  chain sublattice.

TABLE 4. XRD long spacings ( $d_{001}$ ) and short spacings (SS) data for different crystalline thallium(I) hydrogen dialkanoates (molecular associations MCn,<sup>a</sup> for  $9 \leq n \leq 14$ ) at room temperature

MCn	d (Å)					
	$d_{001}$	SS <sup>b</sup>				
9	27.37	4.26s	4.13w	4.00s	3.83m	3.79m
10	30.03	—	4.15w	4.00m	3.81m	3.70s
11	32.53	4.27s	4.15w	4.03w	3.88m	3.78m
12	35.12 <sup>d</sup>	4.22s	4.14w	4.02w	3.84m	3.78m
13	37.63	4.29s	—	4.02m	3.84w	3.73m
14	40.26 <sup>d</sup>	4.29s	—	—	3.88m	3.77m

<sup>a</sup>n indicates the number of carbon atoms in the acid and salt acyl chains.

<sup>b</sup>Intensity: s, strong; m, medium; w, weak.

<sup>c</sup>Hidden by strong long spacing reflections.

<sup>d</sup>35.10 and 40.23 for the respective MC crystallized from ethanol.

Bragg (long) spacing linear ratios corresponding to a one-dimensional lamellar structure. The interlamellar spacings  $d_{001}$  obtained (average values with typical standard deviations of 0.04 Å for  $n = 20$ ) are given in Table 4. As it is known from the work of Piper (25) on potassium acid soaps, the observed MC spacings (35.12 Å for MC12 at room temperature) were distinct from both of their single constituents (30.6 Å or 27.3 Å for the forms B or C, respectively, of the lauric acid, and 30.3 Å for the phase III of the TI laurate at room temperature). A high number of reflections in the wide angle region (short spacings) were also presented, as shown in Table 4 for all the crystalline molecular associations from MC9 (pelargonic-pelargonate) to MC14 members.

## DSC

Slow cooling rates were used in order to obtain the stable solid forms, and slow heating rates were used to facilitate polymorphic transformations; better resolution was gained in those samples capable of being encapsulated in the crystalline state, especially when prepared from ethanol. Proper cooling curves detected only typical supercooling effects. Hysteresis was not exhibited between first and successive runs of stable samples either crystallized from ethanol or cooled from the melt. No exothermic events were observed on heating. Typical DSC heating traces at 1 K/min are shown in Fig. 6 and the thermal data obtained, temperatures T(K), enthalpies  $\Delta H$  (kJ/mol), and the corresponding entropies  $\Delta S$  (J/mol·K), are shown in Table 5.

The equimolar physical mixture of the acid and salt components of a molecular compound exhibited a particularly relevant thermal behavior. The DSC heating curve from an appropriate temperature upwards records the pertinent solid–solid transitions of the pure salt and then the fusion of the pure acid, which, as soon as it appears, begins to be counteracted by an exother-

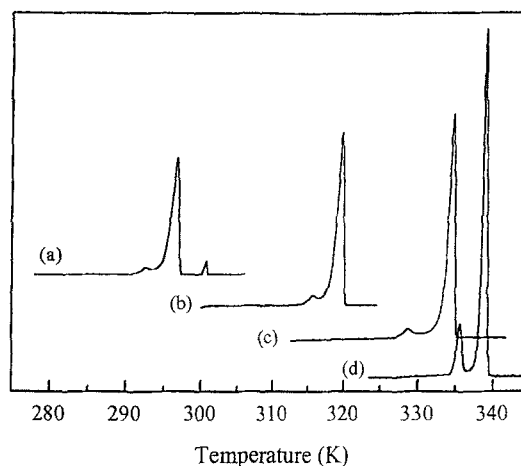


Fig. 6. Heating DSC traces at 1 K/min for different thallium(I) hydrogen dialkanoates: (a) diheptanoate, MC7; (b) dicaprate, MC10; (c) ditridecanoate, MC13; (d) dimyristate crystallized from ethanol, MC14.

mic reaction followed by the melting peak of the corresponding molecular association. DSC traces of subsequent cooling–heating cycles are completely reversible, recording solely the solidification–melting effects of the molecular association, with no trace assignable to the individual behavior of the single components present.

## DISCUSSION

### Nature of the association

The irreversible association becomes quite evident from the previously described DSC behavior of the equi-

TABLE 5. Thermodynamic data of phase transitions for the thallium(I) hydrogen dialkanoates (molecular associations MCn,<sup>a</sup> for  $3 \leq n \leq 14$ ): temperature, T(K); enthalpy,  $\Delta H$  (kJ/mol); entropy,  $\Delta S$  (J/mol·K)

Molecular Association	Crystal/Crystal Transition			Peritectic Fusion		
	T <sub>i</sub>	$\Delta H$	$\Delta S$	T <sub>i</sub>	$\Delta H$	$\Delta S$
MC3	235.2	0.71	3.00	251.7	10.68	42.45
MC4	245.7	1.85	7.53	256.8	17.06	66.44
MC5	255.3	2.44	9.56	264.6	20.97	79.25
MC6	270.5	3.16	11.68	283.5	29.37	103.60
MC7	284.0	3.83	13.47	295.5	34.09	115.36
MC8	298.1	4.57	15.34	307.0	38.27	124.66
MC9	307.0	5.60	18.24	313.6	43.69	139.32
MC10	317.4	6.38	20.19	322.2	50.66	157.23
MC11	322.1	7.23	22.35	327.3	59.22	180.93
MC12	328.9	7.95	24.18	332.7	66.05	198.53
MC13	332.8	8.78	26.38	336.2	72.82	216.54
MC14	336.0	9.59	28.54	339.7	79.10	232.85

<sup>a</sup>n indicates the number of carbon atoms in the acid and the salt acyl chains.

molar acid and salt physical mixture. Consistent with this fact, the vibrational IR and Raman (less apparently) spectra of a crystalline molecular association of the series studied are always different from the composite spectrum calculated for the mechanical mixture of the components in equimolar proportions (Figs. 3 and 5). In a similar manner, the powder X-ray diffractogram of a crystalline molecular association is unique and different from the diffractograms of its constituents. This defines these molecular associations as real chemical species, equimolecular compounds whose existence and characterization are here reported for first time.

The FTIR traces of crystalline equimolecular compounds changed at temperatures near DSC melting points (Fig. 4). New broad absorption bands appeared centered around 2900, 2450, and 1900  $\text{cm}^{-1}$ . Simultaneously, the broad and strong absorption bands corresponding to the nonequivalent carbonyl groups (probably due to a  $\text{Tl}^+$  asymmetric location in the crystalline MCs), at ca. 1685, 1625, and 1550  $\text{cm}^{-1}$  in MC12, are replaced by a new series of bands. At higher frequencies, the new absorptions correspond to  $\nu(\text{C}=\text{O})$  characteristic modes in the acid component (1705 $^{-1}$  in lauric acid). At lower frequencies, the bands correspond to  $\nu_a(\text{COO})$  in the neutral salt (1545 and 1505  $\text{cm}^{-1}$  in Tl laurate), and to  $\nu(\text{C}-\text{O})$  stretching and  $\delta(\text{OH})$  out of plane deformation modes typical of carboxylic acid dimers (ca. 1300 and 950  $\text{cm}^{-1}$ , respectively). Hydrogen bonding studies based on IR data have largely shown (26, 27) that systems with moderate-to-strong H-bonds exhibit three bands (A, B, C), centered around 2900, 2500 and 1900  $\text{cm}^{-1}$ , whilst a single continuous absorption centered at lower frequencies (D band) is observed in very-strong H-bonding systems. The origin of A, B, and C bands is the  $\nu(\text{OH})$  vibration mode in Fermi resonance with  $2\delta(\text{OH})$  and  $2\gamma(\text{OH})$  modes, as in carboxylic acid dimers (28), and that of the D band corresponds to the  $\nu(\text{OH})$  vibration of systems with a very short, symmetric “ $\text{O} \cdots \text{H} \cdots \text{O}$ ” bond (29). Thus IR spectroscopy clearly indicates very strong hydrogen-bonding as responsible for the association between acid (carboxylic OH) and neutral salt (carboxylate O).

The Raman spectra of the molecular compounds showed a broad, very weak feature centered at about 1610–1620  $\text{cm}^{-1}$  (1615 for MC14), very close to the bands observed in IR for  $\nu_a(\text{COO})$  stretching modes. The diffuse feature appears shifted towards lower frequencies with respect to the stronger band of the acid (1632 for myristic acid) but at higher frequencies than the neutral salt (1540 for Tl myristate). Thus Raman data, like IR but more subtly, clearly also support a very strong hydrogen-bonding for the MC compounds. On the other hand,  $^1\text{H}$  and  $^{13}\text{C}$ -NMR spectra of the molecu-

lar compounds in solution were also consistent with a very strong H-bonding. No matter the NMR type, the two  $\beta$  methylenes of any molecular compound present a single signal, which appears intermediate between the respective signals of the corresponding acid and salt components. This is also the case for the two  $\alpha$  methylenes and, in carbon NMR spectra, for the carbonyls couple as well. Thus the two acyl chains to which each pair of moieties belongs are chemically equivalent and, for that, the acid and salt acyl chains have to be associated within the same molecular identity. Finally, as the carboxylic proton experiences downfield shifting, the association has to be stronger than in dimeric acids. In addition, the equimolar physical mixture and the equimolecular association always exhibited identical traces in both kinds of NMR spectra, but always distinct from those of both constituents, indicating that this chemical species can be spontaneously formed and exists in proper solvent media.

Phase diagram investigations carried out on the normal series of thallium(I) alkanolate + alkanolic acid binary systems (19, 30) definitely demonstrate that this molecular compound in the 1:1 stoichiometric ratio,  $(\text{TlO}_2\text{C}(\text{CH}_2)_{n-2}\text{CH}_3) \cdot (\text{HO}_2\text{C}(\text{CH}_2)_{n-2}\text{CH}_3)$  for  $3 \leq n \leq 14$ , thallium(I) hydrogen dialkanoates (acid thallium(I) alkanolates, fatty acid thallium(I) soaps), is the only stable association detected, making the Tl(I) behavior similar to the K, in contrast to that of the Na-related systems (19). It seems that the counterion size determines by steric effects whether the molecular association may occur with several stoichiometries (when relatively small) or equimolecularly only (when relatively big).

### Hydrocarbon chain packing

In comparison to both acid and salt, the acid soaps showed an enhancement in the intensity of the  $w(\text{CH}_2)$  wagging progression bands in the IR 1100–1330  $\text{cm}^{-1}$  region (in number of  $(n+1)/2$  or  $n/2$  for odd or even acids and carboxylates), indicating a relatively higher crystallinity for the hydrocarbon chains in the room temperature MC. Raman bands around 1300  $\text{cm}^{-1}$ ,  $t(\text{CH}_2)$  twisting mode, and at ca. 1120 and 1060  $\text{cm}^{-1}$ ,  $\nu(\text{CC})$  skeletal modes, remain strong and sharp in the three chemicals (acid plus salt mixture, and molecular association MC14 in Fig. 5), meaning that the alkyl chains are in a similar all-*trans* conformation throughout, though packing modes may be different.

The factor group splitting in the first term ( $k=0$ ) of the  $r(\text{CH}_2)$  rocking progression bands around 720  $\text{cm}^{-1}$  (720 and 728 for MC12), and  $\delta(\text{CH}_2)$  scissoring mode near 1460  $\text{cm}^{-1}$  (1465 and 1470 for MC12), recorded in the IR spectrum of all the samples at the lowest temperature, suggest (31) that the crystalline acid soaps present an orthorhombic symmetry in their chain

TABLE 6. Intensity ratios for Raman absorption bands of the  $\delta(\text{CH}_2)$  scissoring and  $\nu(\text{CH})$  stretching modes in solid thallium(I) hydrogen dialkanoates (molecular associations  $\text{MC}_n$ ,<sup>a</sup> for  $9 \leq n \leq 14$ )

Molecular Association	$R_2 = \frac{I(1460)}{I(1440)}$	$R_3 = \frac{I(2850)}{I(2880)}$
MC9, pelargonic-pelargonate <sup>b</sup>	0.67	0.46
MC10, capric-caprate	0.68	0.51
MC11, undecanoic-undecanoate	0.68	0.51
MC12, lauric-laurate <sup>b</sup>	0.65	0.48
MC13, tridecanoic-tridecanoate	0.68	0.51
MC14, myristic-myristate	0.69	0.51
$\beta$ (T  ) Triglycerides <sup>c</sup>	0.84	0.45
$\beta'_1$ (O $\perp$ ) Triglycerides <sup>c</sup>	0.58	0.54
$\beta'_2$ (O $\perp$ ) Triglycerides <sup>c</sup>	0.65	0.62
$\alpha$ (O  ) Triglycerides <sup>c</sup>	0.67	0.69

<sup>a</sup>n indicates the number of carbon atoms in the acid and the salt acyl chains.

<sup>b</sup>Low values may result if solid solutions with the salt are present (usually detected by DSC but not by IR and XRD).

<sup>c</sup>From ref. 35;  $R_2 = I(1460)/I(1438)$ ;  $R_3 = I(2858)/I(2880)$ .

arrangement with two alkyl chains interacting in the subcell, O $\perp$  chain packing.

The crossed chain configuration is confirmed by the Raman spectra in the range of 1400–1500  $\text{cm}^{-1}$ , particularly with the presence of a sharp band at around 1416–1420 (1419 for MC14), also associated with a split component of the  $\delta(\text{CH}_2)$  scissoring mode at about 1440 and 1460 (1441 and 1457 for MC14), which is a specific characteristic of this type of orthorhombic perpendicular chain subcell in different kinds of lipids (32–34), including long-chain alkanes and phospholipid–water gels. The  $\nu(\text{CH})$  stretching region of 2800–3000  $\text{cm}^{-1}$  is also sensitive to the subcell type, and the pattern shown in Fig. 5 for MC14 corresponds to the O $\perp$  chain packing mode (34). Furthermore, the different polymorphic forms of a given lipid seem to exhibit characteristic Raman vibrational band ratios, due to specific chain–chain interactions, which have been used in phase identification, as shown in Table 6 where data on the equimolecular compounds series are compared with those collected for saturated monoacyl triglycerides (35). Note that  $R_3$  values are around 0.51, close to that of  $\beta'_1$ -triglycerides, whilst  $R_2$  values are around 0.68, closer to that of  $\beta'_2$ -triglycerides this time, but thallium(I) hydrogen dialkanoates may exhibit their distinct characteristic ratios.

On the other hand, the XRD short spacing patterns obtained for the MC series are related with an orthorhombic perpendicular type of hydrocarbon chain subcell. Thus, consistent with the vibrational spectroscopic behavior, these MC compounds can be characterized as a sort of  $\beta'$ -phase in the nomenclature of Larsson for glyceride polymorphism (36), as a pure short spacings pattern is not exactly matched. Actually, the short spacing reflections appear as fine sharp bands in a sort of

double set as if two coexistent pseudo- $\beta'_2$  and pseudo- $\beta'_1$  modifications were present (33, 37, 38) in the room temperature MC solids (coexistence of two or more solid phases is frequently observed in lipid crystallization). The phases would differ in the lateral, intermolecular packing arrangement of the hydrocarbon chains but conserve the common orthorhombic perpendicular symmetry, so that only slight differences would be derived in the unit subcell dimensions without practical alteration of the molecular structure (33) as XRD long spacings never exhibit double pattern. Consequently, the pseudo- $\beta'_2$  phase would appear in a narrow temperature range immediately below the melting point of the high-temperature pseudo- $\beta'_1$  phase, and the polymorphic pseudo- $\beta'_2 \rightarrow$  pseudo- $\beta'_1$  transformation would occur reversibly with minor thermodynamic changes (33), as is observed in the thermal behavior of all MC members. Whether this phenomenon results from a pseudo- $\beta'_2$  phase alone or in coexistence with a pseudo- $\beta'_1$  phase could not be ascertained because of failure to isolate the latter form from either the solvent or the melt.

### Compound structures

Raman spectra at low frequency (not covered in Fig. 5) show the presence of a weak feature at a frequency of about 75  $\text{cm}^{-1}$  in all the crystalline acid soaps that does not change in a continuous way with the chain carbon atoms number, as in normal alkanes, but remains constant as in the corresponding neutral TI carboxylates, which seem to be associated with the big thallium mass (39). This weak feature appears close to the LAM-1 band observed in the corresponding carboxylic acid dimers (40), indicating that the arrangement of MC chains must be very similar to that in the bilayer lamellae of the dimeric acids.

XRD traces displaying a high number of sharp reflections in both low and wide angle regions indicate, confirming vibrational spectroscopic data, that the equimolecular compounds really show a well-organized lamellar structure at room temperature with both layer and chain packing orders. The long spacings  $d_{001}$  that were obtained (Table 4) vary linearly with the number (n) of carbon atoms in each acid and soap acyl chain (correlation coefficient  $R = 0.99997$ , standard deviation of the estimation (SD) = 0.04), indicating that the room temperature compounds probably belong to an isomorphic structural homologous series. This regression coefficient (increment of the lamellar thickness per  $\text{CH}_2$  group in each acyl chain) was  $2.57 \pm 0.01 \text{ \AA}$  which, assuming 1.53  $\text{Å}$  and  $112^\circ$  for the C–C bond in the all-*trans* conformation, strongly suggests that the alkyl chains are essentially aligned at an angle of  $90^\circ$  with respect to the lamellar basal plane. Thus the lamellar structure consists of a single molecule array where the alkyl chains are vertically aligned up and down to the



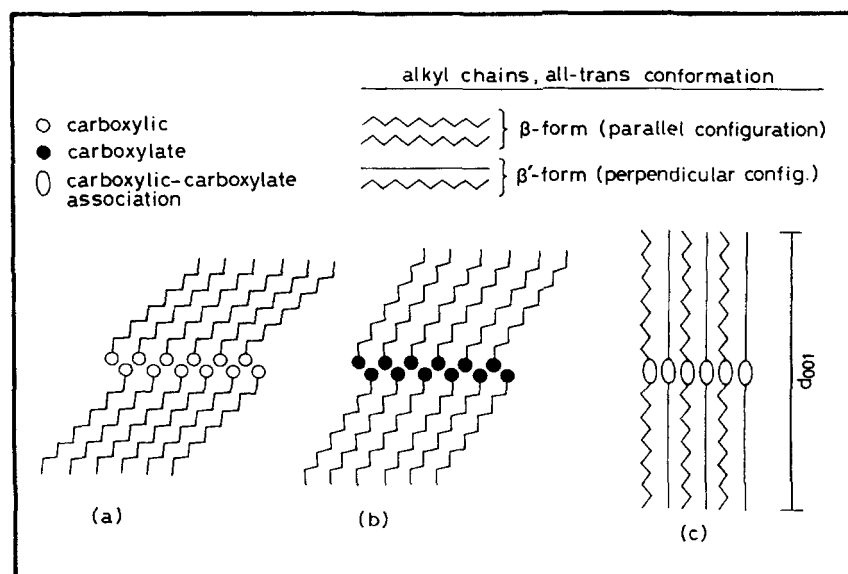


Fig. 7. Schematic representation of lamellar structures: (a) alkanolic acid; (b) thallium(I) alkanolate; (c) thallium(I) hydrogen dialkanolate.

“cation/hydrogen bond” network in an all-*trans* conformation and orthorhombically arranged in intermolecular crossed configuration (mutually perpendicular orientation), in a methyl-to-methyl arrangement, as shown in Fig. 7.

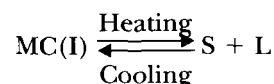
Extrapolation of the linear fit for  $n = 2$  (acetic-acetate MC2) gives  $d_{001} = 9.44 \text{ \AA}$  which, considering  $4 \text{ \AA}$  as a rough contribution of the two terminal methyl groups to the all-*trans* alkyl chain length taken from normal alkanes, yields a thickness of around  $5.5 \text{ \AA}$  for the  $\text{TlCOO} \cdot \text{HOOC}$  polar network of the Tl acid soaps lamellae. These data compare well with that of  $5\text{--}6 \text{ \AA}$  given for the  $\text{KCOO} \cdot \text{HOOC}$  association in the vertical forms of equimolecular potassium acid soaps (7), the only precedent in the literature. On the other hand, the absorption continuum, B band from  $\nu(\text{OH})$  stretching vibrations is centered around  $1100\text{--}1400 \text{ cm}^{-1}$  which allows (41) an estimate of about  $2.48\text{--}2.51 \text{ \AA}$  for the  $\text{O} \dots \text{O}$  distance in the MC12, in agreement with the calculated and crystallographically measured value of  $2.48 \text{ \AA}$  for potassium acid diacetate (40). Interestingly, it is possible to compare  $d_{001}$  lamellar distances of isomorphous vertical forms for the same members of different acid soaps homologous series; i.e., for the acid laurates of Na, K, and Tl the corresponding  $d_{001}$  values are  $35.76$ ,  $35.53$  (both from ref. 25) and  $35.12 \text{ \AA}$ , respectively. Thus the acid soap lamellar thickness decreases slightly in spite of the increasing cation size ( $0.95$ ,  $1.33$ , and  $1.40 \text{ \AA}$  for the respective ionic radii). If the same chain length is assumed for the same all-*trans* vertical forms, the  $\text{MeCOO} \cdot \text{HOOC}$  polar network will be the molecular fragment enduring this length reduction and, correspondingly, the hydrogen bond of the acid

soap will become stronger in the  $\text{Na}^+ < \text{K}^+ < \text{Tl}^+$  sequence. This, in principle, is not obvious but, in the final analysis, it would mean that the bigger the cation, the smaller steric perturbation the cation and the carboxylic-carboxylate moiety will undergo. Assuming that the H-bond moieties are planar and linked together by the interposition of the metal cation (coordination) to give infinite three-dimensional sequences, the bigger the cation, the looser the packing will be. All this could justify the differences found in the  $1500\text{--}1800 \text{ cm}^{-1}$  IR region of the sodium hydrogen didodecanoate (8) with respect to the present thallium derivative, as well as the already mentioned fact of the various stoichiometries for the sodium against the single equimolar association for the thallium acid soaps.

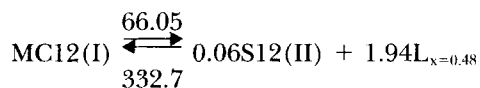
#### Phase transitions: thermodynamic data

The MC compounds always present a small endotherm (Fig. 6) around  $8$  to  $15$  degrees prior to the main melting peak, due to the  $\text{MC(II)}/\text{MC(I)}$  crystal/crystal transition (pseudo- $\beta_2' \rightarrow$  pseudo- $\beta_1'$  transformation), which in the MC12 takes place at  $328.9 \text{ K}$  with a transition enthalpy of  $7.95 \text{ kJ/mol}$ , and an entropy gain of  $24.18 \text{ J/mol}\cdot\text{K}$ . Table 5 contains all the thermal information.

FTIR thermal data have been shown clearly pointing to this crystalline association breaking down into its constituents on melting. Polarized microscopy observations and DSC data specifically confirm a peritectic type of melting, represented by the following equilibrium,



where S is the corresponding salt stable at the melting temperature in the polymorphic phase indicated by roman numerals in parentheses, i.e., S(III) for MC3, MC4, MC5, MC6 and MC9, S(II) for MC7, MC10, MC11, MC12, MC13 and MC14, and S(I) for MC8. L is an acid + salt liquid phase of the peritectic composition, close to 0.48–0.49 salt molar fraction in all the cases studied. In the lauric-laurate association MC12, referred to one mol of molecular compound,



where thallium(I) laurate S12 solid phase II and the melt L (lauric acid:thallium laurate in around 1.1:1 molar ratio) are the peritectic reaction products with the respective stoichiometric coefficients of 0.06 and 1.94. The parameters indicated above and below the equilibrium arrows are the endothermal molar enthalpy of melting  $\Delta_f H$  (kJ/mol) and the isothermal melting temperature  $T_f$  (K), respectively; so that the peritectic reaction takes place at 332.7 K with 66.05 kJ/mol of energy consumption, and an entropy increase of 198.53 J/mol·K.

One relevant point concerning the IR thermal behavior still remains to be discussed, i.e., at the corresponding DSC melting temperatures the strong and sharp wagging and rocking progression bands due to the crystalline polymethylene chains smear into broad ones and the fine structure practically disappears. This fact clearly points to the peritectic melting as a cooperative process of simultaneous conformational chain disorder (liquid-like state) and hydrogen bond breaking. The melting mechanism is then opposite to the case of their parent neutral Tl alkanooates where the transit from the crystal stable at the lowest temperature up to the isotropic liquid takes place in a stepwise fashion through an extensive polymorphism and mesomorphism plus a non-cooperative process of chain melting (39).

Comparing the phase transition thermodynamics of the MC compounds to other kinds of lipid homologous series, it is interesting to note the pattern that the relevant thermodynamic data follow as the alkyl chain length increases. The melting temperatures  $T_f$  do not alternate in spite of the OL subcell because the perpendicularity of the hydrocarbon chains to the lamellar basal plane yields the same structure for the methyl terminal planes in all the MC members with either odd or even acyl chains. Thus the interfaces between lamellae always present the same packing density and identical lamellar stacking results in all the vertical forms of the MC homologous members of the series. Hence nonalternation follows correspondingly. The polymorphic pseudo- $\beta'_2$ /pseudo- $\beta'_1$  transition temperatures  $T_f$  do not alternate either, and seem to be a stable

situation as convergence to the melting points, and subsequent single  $\beta'$ -phase existence, would take place at very high chain lengths.

The polymorphic transition enthalpies  $\Delta_f H$  range around 1–10 kJ/mol, increasing very smoothly with chain length  $n$ , whilst molar enthalpies of fusion  $\Delta_f H$  are highly dependent (correlation coefficient better than 0.997), with an averaged slope of 6.20 kJ/mol. These data, i.e., 3.10 kJ/mol per methylene group when total carbon atoms in the MC chains are considered, are somewhat low in relation to that of 3.89 kJ/mol reported for the fusion of  $\beta'$ -forms in triglycerides (35). Notwithstanding, this peritectic fusion of the thallium acid soaps comprises about 90% of the total enthalpic increments that both constituents, alkanooic acid and thallium alkanooate, experience over near 300 degrees through several polymorphic transitions, their fusion, and the thermotropic mesomorphism and clearing of the salt.

The chain segments of long-chain flexible molecules, such as normal aliphatic hydrocarbons and their substitution derivatives (alcohols, carboxylic acids, esters, etc.), execute torsional oscillations in the crystal and hindered rotations relative to each other in the liquid. The corresponding theoretical increments per chain link ( $\text{CH}_2$  group) in the enthalpy and entropy thermodynamic functions are rather constant estimations, namely  $R/2$  and  $R \cdot \ln 3$ , respectively (42),  $R$  being the gas constant. According to pertinent literature (43, 44), the melting of normal alkanooic acids records an enthalpy gain of  $0.49R$  per methylene group for both even ( $8 \leq n \leq 20$ ) and odd ( $11 \leq n \leq 19$ ) members, whilst  $1.26R$  and  $1.24R$  are the respective entropy increments. On the other hand, experimental data collected over approximately 500 degrees from 4–6 K, on the homologous series of normal thallium(I) alkanooates from propanoate to tetradecanoate (45), show that cooperative effects involve less than 50% of the theoretical increments per methylene link quoted above for the melting process of flexible molecules. It was further observed that the morphology of the heat capacity/temperature curve exhibited a rather subtle and uncommon phenomenon in all the cases, consisting of an anomalous enhancement extended over very wide temperature intervals, that was finally interpreted (39) as a non-cooperative effect associated with the melting of the aliphatic chains. When this conformational disordering contribution is also taken into account, the computed increments per methylene group rise to  $0.51R$  and  $1.35R$  for the respective enthalpy and entropy of melting of the even members ( $n \leq 14$ ) of neutral Tl alkanooates (J. A. R. Cheda, F. L. López de la Fuente, M. V. García, M. I. Redondo, F. Fernández-Martín, and E. F. Westrum, Jr., unpublished results).

Note that the peritectic melting of the MC com-

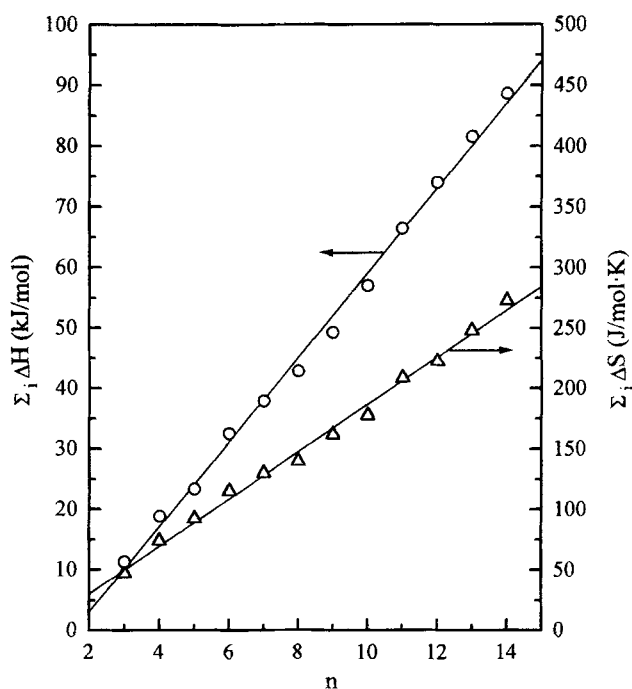



**Fig. 8.** Experimental thermal data on the thallium(I) hydrogen dialkanoates for the entire solid→liquid process, as a function of carbon atoms number  $n$  in the acid and salt acyl chain: (circles) enthalpies,  $\Sigma_i\Delta H$  (kJ/mol); (triangles) entropies,  $\Sigma_i\Delta S$  (J/mol · K); (solid lines) regression fits.

pounds yields the respective neutral salt that, depending on the phase diagram of the acid + salt binary system concerned, may experience a crystal/crystal transition along its heterothermal melting (dissolution into the melt), as shown in Fig. 6(a) for the diheptanoate MC7. These two contributions are rather small and already included in the main peak of the MC $n$  members with even  $n$  ( $\Delta_f H$  in Table 5) as their closeness did not enable them to be separately recorded, but as a smooth hump on the main DSC trace declining arm. They range about 0.1–0.5 and 0.5–2 kJ/mol, respectively, and should also be taken into account for calculating the total enthalpy  $\Sigma_i\Delta H$  and total entropy  $\Sigma_i\Delta S$  changes associated with all the thermal transformations,  $i$ , that complete the entire transit of the MC members from the polymorph stable at the lowest temperature up to the whole isotropic liquid. Both sets of data,  $\Sigma_i\Delta H$  and  $\Sigma_i\Delta S$ , evolve linearly with chain length  $n$ , as can be seen in Fig. 8 where experimental results are given alongside their regression fits.

The regression analysis carried out yielded correlation coefficients better than 0.997 in both cases, the regression coefficients being 7.00 kJ/mol and 19.55 J/mol · K, respectively, equivalent to the dimensionless figures of 0.42R and 1.18R per methylene group of the total chain length. These contributions per  $\text{CH}_2$ -group in the thallium(I) hydrogen dialkanoates represent

about 80–85% of those determined for the normal alkanic acids and the neutral thallium(I) salts. The central rigid-molecule fragment, Tl-cation/H-bond network of the thallium(I) hydrogen dialkanoates should introduce some extra restriction for the connected flexible alkyl chains to torsional oscillation in the crystal but, once it peritectically disappears, should not represent any additional rotation hindrance in the liquid. However, the IR spectrum of MC12 just above the melting point, Fig. 4, indicates the existence of stronger interactions (A, B, C bands) than in the case of the corresponding acid dimers melt. Both constrictions imply that the empirical values regarding the enthalpy and entropy changes at the melting point must undergo some kind of reduction, and the data quoted above may represent quite reasonable estimates for the series of thallium(I) hydrogen dialkanoates.

Finally, it seems worthwhile to remember that some of these thallium acid soaps reversibly melt at ordinary temperatures,  $\pm 20^\circ\text{C}$  around room temperature, with a very important heat of melting, around 20–45 kJ/kg, which enables them to be considered as potential thermal energy storage materials. 

Manuscript received 7 June 1996 and in revised form 7 November 1996.

## REFERENCES

1. McBain, J. W., and M. C. Field. 1933. Phase rule equilibria of acid soaps. I. Anhydrous acid potassium laurate. *J. Phys. Chem.* **37**: 675–684.
2. Lucassen, J. 1966. Hydrolysis and precipitates in carboxylate soap solutions. *J. Phys. Chem.* **70**: 1824–1830.
3. Ekwald, P., and L. Mandell. 1969. Solutions of alkali soaps and water in fatty acids. I. Region of existence of the solutions. *Kolloid-Z. Polym.* **233**: 938–944.
4. Friberg, S., L. Mandell, and P. Ekwald. 1969. Solutions of alkali soaps and water in fatty acids. III. IR and NMR investigations. *Kolloid-Z. Polym.* **233**: 955–962.
5. Cistola, D. P., D. Atkinson, J. A. Hamilton, and D. M. Small. 1986. Phase behavior and bilayer properties of fatty acids: hydrated 1:1 acid-soaps. *Biochemistry.* **25**: 2804–2812.
6. Stenius, P., and P. Ekwald. 1980. Formation of lyotropic liquid crystals by organic salts. In *Thermodynamic and Transport Properties of Organic Salts*. IUPAC Chemical Data Series, Vol. 28. F. Franzosini and M. Sanesi, editors. Pergamon Press, London. 321–339.
7. Small, D. M. 1986. The Physical Chemistry of Lipids from Alkanes to Phospholipids. *Handbook of Lipid Research Series*. Vol. 4. D. H. Hanahan, editor. Plenum Press, New York. 332–338.
8. Mantsch, H. H., S. F. Weng, P. W. Yang, and H. H. Eysel. 1994. Structure and thermotropic phase behavior of sodium and potassium carboxylate ionomers. *J. Mol. Struct.* **324**: 133–141.
9. McBain, J. W., and M. C. Field. 1933. Phase-rule equilibria of acid soaps. Part II. Anhydrous acid sodium palmitates. *J. Phys. Chem.* **37**: 920–924.

10. Ryer, F. V. 1946. Acid sodium stearates. *Oil & Soap*. **9**: 310–313.
11. Pacor, P., and H. L. Spier. 1968. Thermal analysis and calorimetry of some fatty acid sodium soaps. *J. Am. Oil Chem. Soc.* **45**: 338–342.
12. Brouwer, H. W., and W. Skoda. 1969. Calorimetric, dilatometric and microscopic investigations of the system sodium stearate-stearic acid. *Kolloid-Z. Polym.* **234**: 1138–1147.
13. Brouwer, H. W., and H. L. Spier. 1971. Acid-soap formation in various anhydrous sodium soaps. *Proc. Int. Conf. Thermal Anal., 3rd*. **3**: 131–144.
14. Trzerowski, N. 1976. Interactions on sodium soaps/fatty acid systems. *Wiss. Ztschr. Friedrich-Schiller-Univ. Jena, Math.-Nat. R.* **25**: 891–899.
15. McBain, J. W., and A. Stewart. 1933. Phase-rule equilibria of acid soaps. Part III. Anhydrous acid potassium oleate. *J. Phys. Chem.* **37**: 924–928.
16. Goddard, E. D., S. Goldwasser, G. Golikeri, and H. C. Kung. 1968. Molecular association in fatty acid-potassium soap systems. *Adv. Chem. Ser.* **84**: 67–77.
17. Kung, H. C., and E. D. Goddard. 1969. Molecular association in fatty acid potassium soap systems. II. *J. Colloid Interface Sci.* **39**: 242–249.
18. Sanesi, M., A. Cingolani, P. L. Tonelli, and P. Franzosini. 1980. Thermal properties. In *Thermodynamic and Transport Properties of Organic Salts*. IUPAC Chemical Data Series. Vol. 28. F. Franzosini and M. Sanesi, editors. Pergamon Press, London. 29–117.
19. Fernández-García, M. 1989. Diagrama de fases del sistema binario Acido heptanoico y Heptanoato de talio(I). M.D. Thesis. Facultad Químicas, Universidad Complutense. Madrid.
20. Fernández-Martín, F., M. Fernández-García, and J. A. R. Cheda. 1990. (Thallium alkanooates + alkanooic acids) interactions: molecular association, polymorphism and mesomorphism. Plenary Lecture. 12th Convegno Naz. Calorimetrie Anal. Termica, Bari (Italy).
21. Laban, A. K., F. L. López de la Fuente, J. A. R. Cheda, E. F. Westrum, Jr., and F. Fernández-Martín. 1989. Thermodynamics of thallium alkanooates. VI. Thallium(I) heptanoate revisited. *J. Chem. Thermodynamics*. **21**: 375–384.
22. Hopkins, C. Y., and H. J. Bernstein. 1959. Applications of proton magnetic resonance spectra in fatty acid chemistry. *Can. J. Chem.* **37**: 775–782.
23. Hopkins, C. Y. 1961. Nuclear magnetic resonance in lipid analysis. *J. Am. Oil Chem. Soc.* **38**: 664–668.
24. Malkin, T. 1952. The molecular structure and polymorphism of fatty acids and their derivatives. *Prog. Chem. Fats Other Lipids*. **1**: 6–7.
25. Piper, S. H. 1929. An X-ray examination of some salts of fatty acids. *J. Chem. Soc.* 234–239.
26. Hazdi, D., and S. Bratos. 1976. Vibrational spectroscopy of the hydrogen bond. In *The Hydrogen Bond*. P. Schuster, G. Zundel, and C. Sandorfy, editors. North Holland Publishing Co., Amsterdam. 565–611.
27. Emsley, J. 1980. Very strong hydrogen bonding. *Chem. Soc. Rev.* **9**: 91–124.
28. Pelmeshnikov, A. G., J. H. M. C. van Wolput, J. Yanchen, and R. A. van Santen. 1995. (A,B,C) triplet of infrared OH bands of zeolitic H-complexes. *J. Phys. Chem.* **99**: 3612–3617.
29. Yukhnevich, G. V., E. G. Tarakanova, V. D. Mayorov, and N. B. Librovich. 1992. Theoretical study of the short asymmetric (O ··· H ··· O) hydrogen bond in solid potassium hydrogen diformate. Including electron correlation. *J. Mol. Struct.* **265**: 237–267.
30. Cheda, J. A. R., M. Fernández-García, P. Ferloni and F. Fernández-Martín. 1991. (Thallium(I) tetradecanoate + tetradecanoic acid) phase diagram: formation of a molecular complex. *J. Chem. Thermodynamics*. **23**: 495–502.
31. Chapman, D. 1962. The polymorphism of glycerides. *Chem. Rev.* **62**: 433–456.
32. Simpson, T. D., and J. W. Hagemann. 1982. Evidence of two  $\beta'$  phases in tristearin. *J. Am. Oil Chem. Soc.* **59**: 169–171 (and references therein).
33. Sato, K., T. Arishima, Z. H. Wang, K. Ojima, N. Sagi, and H. Mori. 1989. Polymorphism of POP and SOS. I. Occurrence and polymorphic transformation. *J. Am. Oil Chem. Soc.* **66**: 664–674.
34. Kobayashi, M. 1988. Vibrational spectroscopic aspects of polymorphism and phase transition of fat and fatty acids. In *Crystallization and Polymorphism of Fats and Fatty Acids*. N. Garti and K. Sato, editors. Marcel Dekker, Inc., New York. 146–152.
35. Hagemann, J. W. 1988. Thermal behavior and polymorphism of acylglycerides. In *Crystallization and Polymorphism of Fats and Fatty Acids*. N. Garti and K. Sato, editors. Marcel Dekker, Inc., New York. 18–27.
36. Larsson, K. 1968. Classification of glyceride crystal forms. *Acta Chem. Scand.* **20**: 2255–2260.
37. Hernqvist, L., and K. Larsson. 1982. On the crystal structure of the  $\beta'$ -form of triglycerides and structural changes at the phase transitions  $Liq. \rightarrow \alpha \rightarrow \beta' \rightarrow \beta$ . *Fette Seifen Anstrichm.* **84**: 349–354.
38. Hernqvist, L. 1988. Crystal structures of fats and fatty acids. In *Crystallization and Polymorphism of Fats and Fatty Acids*. N. Garti and K. Sato, editors. Marcel Dekker, Inc., New York. 123–135.
39. García, M. V., M. I. Redondo, F. L. López de la Fuente, J. A. R. Cheda, E. F. Westrum, Jr., and F. Fernández-Martín. 1994. Temperature dependence of the vibrational spectra of thallium(I) alkanooates. *Appl. Spectrosc.* **48**: 338–344.
40. Minoni, G., and G. Zerbi. 1982. End effects on longitudinal accordion modes: fatty acids and layered systems. *J. Phys. Chem.* **86**: 4791–4798.
41. Novak, A. 1974. Hydrogen bonding in solids. Correlation of spectroscopic and crystallographic data. In *Structure and Bonding* 18. J. D. Dumtz, P. Hemmerich, R. H. Holm, J. A. Ibers, C. K. Jørgensen, J. B. Neilands, D. Reinen, and P. J. P. Williams, editors. Springer-Verlag, Berlin. 177–217.
42. Bondi, A. 1968. *Physical Properties of Molecular Crystals, Liquids, and Glasses*. John Wiley & Sons, New York. 159–170.
43. Schaake, R. C. F., J. C. van Miltenburg, and C. G. de Kruif. 1982. Thermodynamic properties of the normal alkanooic acids. I. Molar heat capacities of seven odd-numbered normal alkanooic acids. *J. Chem. Thermodynamics*. **14**: 763–769.
44. Schaake, R. C. F., J. C. van Miltenburg, and C. G. de Kruif. 1982. Thermodynamic properties of the normal alkanooic acids. II. Molar heat capacities of seven even-numbered normal alkanooic acids. *J. Chem. Thermodynamics*, **14**: 771–778.
45. Cheda, J. A. R., P. Ungarelli, F. L. López de la Fuente, F. Fernández-Martín, Y. Xu, W. L. Ijdo, and E. F. Westrum, Jr. 1995. Thermodynamics of the thallium alkanooates. IX. Thermodynamics of thallium(I) octanoate from temperatures of 6 to 490 K. *Thermochim. Acta* **266**: 163–173.